J. Chem. Sci., Vol. 121, No. 6, November 2009, pp. 1069–1076.

Disposable amperometric immunosensor based on layer-by-layer electro-depositing of the nanogold particles, prussian blue-modified indium tin oxide for determination of α-fetoprotein

YAN LI[a], WEN-BIN LIANG[b], LI-CHAO FANG[a], HUI HUANG[a], JUN DENG[a] and JUN-SONG ZHENG[a,*]

[a]Department of Clinical Laboratory Science, Third Military Medical University, Gaotanyan Street 30, Shapingba District, Chongqing 400038, P R China

[b]Department of Clinical Biochemistry, Laboratory Sciences, Third Military Medical University, Gaotanyan Street 30, Shapingba District, Chongqing 400038, P R China

e-mail: zhengalpha@yahoo.cn

MS received 23 December 2008; revised 14 August 2009; accepted 7 September 2009

Abstract. In this paper, a novel disposable immunosensor for the detection of α-fetoprotein (AFP) based on the Indium tin oxide (ITO) modified by the sequential electro-deposition of the nanogold particles (nano-Au) and prussian blue (PB) is described. The ITO is employed to reduce the cost, instead of expensive gold electrode, glassy carbon electrode or platinum electrode. The layer-by-layer (LBL) electro-deposition of the nano-Au, PB is used for blocking the possible leakage from the substrate electrode surface and to prevent shedding of composite membrane. Under optimal conditions, the proposed immunosensor displays a broad linear response to AFP, the working range being 0·25 to 300·0 ng mL^{-1} with a detection limit of 0·04 ng mL^{-1}. The studied immunosensor exhibits high sensitivity, fast analytical time and good stability. The proposed methodology is potentially attractive for clinical immunoassays.

Keywords. Indium tin oxide; nanogold particles (nano-Au); α-fetoprotein; layer-by-layer; electrodeposition.

1. Introduction

α-Fetoprotein (AFP), an oncofetal glycoprotein with a molecular weight of about 70 kDa, was most reliably and widely used as a tumor maker for hepatocellular carcinoma (HCC) and often appeared in yolk sac tumor.[1] AFP was normally excreted by the fetal yolk sac, the fetal gastrointestinal tract and eventually by the fetal liver.[2,3] The serum concentration of AFP was relatively high in the embryonic period, but that decreased rapidly after birth and fall to normal adult levels by the first year of life. Also, pregnant women who have high levels of AFP may indicate infants with an abnormal fetal brain or spinal cord.[3,4] Typically, the serum concentration of AFP in healthy adult was less than 25 ng mL^{-1}, and an increasing AFP in the serum may predict high risk at HCC, germ cell tumors, metastatic cancer.[5,6] Recently it has been found that AFP was associated with hepatitis B, hepatitis C, breast cancer and syndrome.[7,8] Hence, the determination of AFP levels in serum played an important role in screening for a disease, diagnosing a disease, and determining the prognosis of a disease.

A number of methods have been reported for the determination of AFP, including fluorescence atomic studies,[9] absorption spectrometry[10] and enzyme-linked immunoassay (ELISA).[11] However, these methods have some limitations such as the radiation hazards, long analysis time, the complicated wash procedure, and expensive and cumbersome instruments. As a result, simple, rapid and sensitive methods to detect AFP in human serum were desirable.

Immunoassays, based on specific antigen-antibody recognition for analytical purposes, have been the excellent analytical methods due to their advantages of inexpensive instrumentation, simple pre-

*For correspondence

treatment procedure, fast analytical time, precise and sensitive current measurements.[12] Conventional signal amplification of the immunoconjugates often was achieved by enzyme labelling of the antigen or antibody, which was relatively expensive and time-consuming.[13] In order to overcome these drawbacks, many high sensitivity and label-free enzyme immunosensors have been described.[14,15]

Because of excellent optical transparency, high electrical conductivity, excellent substrate adhesion, stable electrochemical and physical properties,[16–18] the application of ITO electrodes has attracted increasing interest. In recent years, the development of ITO electrodes and their application to electronic and optical sensors, direct electron transfer of protein, microfluidic on-chip detection, electrochemical nucleic acid biosensors, and electrochemiluminescence analysis have attracted considerable attention.[19–22] In the current work, we developed a novel strategy, which employed the ITO to reduce the cost, instead of expensive gold electrode, glassy carbon electrode or platinum electrode to construct a new disposable amperometric immunosensor with good sensitivity and high stability.

Preparation of gold nanoparticles-modified electrode surfaces generally can be carried out in two ways: electrostatic adsorption and covalent bonding. However, tedious procedures were required to assemble gold nanoparticles on to the electrode surface and the gold nanoparticles layer formed was often unstable. Electro-deposition of gold nanoparticles was a simple and promising method to form a film on an electrode which can then be used to immobilize proteins.[23]

Herein, the immunosensor was prepared by using the LBL electrochemical deposition technique instead of electrostatic adsorption, covalent bonding and LBL assembly to block the possible leakage from the substrate electrode surface and prevent shedding of composite membrane. The immunosensor was fabricated by two steps: first, the nano-Au, PB, and nano-Au was alternately electrochemically deposited onto the ITO surface, which constructed the nano-Au/PB/nano-Au multilayer films by LBL deposition. Then, the alpha-Fetoprotein antibody (anti-AFP) was adsorbed onto the surface of the nano-Au layer and bovine serum albumin (BSA) was used to block possible remaining active sites of the nano-Au monolayer.

Compared with the conventional enzyme immunosensors, this proposed immunosensor has several novelties: such as the ITO was used to reduce the cost. Furthermore, the LBL electrochemical deposition technique was able to enhance the stability of electrode surface and prolong the useful life of this electrode. Tests performed with this immunosensor showed good linearity, sensitivity, specificity and high stability when it was evaluated on several standard serum samples. The electrochemical behaviours and factors influencing the performance of the resulting immunosensors were investigated in detail.

2. Experimental

2.1 *Reagent and materials*

ITO sheets (resistance 100 Ω/sqr) were purchased from Shenzhen Yuanheng (China). AFP antibody and AFP antigen were purchased from Biocell Company (Zhengzhou, China). BSA (96%–99%), gold chloride ($HAuCl_4$) and sodium citrate were obtained from Sigma Chemical Co. (St. Louis, MO, USA). All other materials used were of analytical grade and purchased from Chemical Reagent Company (Chongqing, China). Deionized water was used throughout this research. Phosphate buffered solutions (PBS) were prepared using 0·1 mol L^{-1} Na_2HPO_4, 0·1 mol L^{-1} KH_2PO_4 and 0·1 mol L^{-1} KCl. The prepared solutions were kept at 4°C before use. Au colloids were produced by reducing $HAuCl_4$ with sodium citrate at 100°C for half an hour.[24,25]

2.2 *Apparatus*

Cyclic voltammetric (CV) measurements were performed on a CHI 660a electrochemistry workstation (Shanghai CH Instruments, China) with a three-electrode system contained a platinum wire auxiliary electrode, a saturated calomel reference electrode (SCE) and the bare or modified ITO electrode as working electrode. The pH measurements were made with a pH meter (MP 230, Mettler-Toledo, Switzerland) and a digital ion analyzer (Model PHS-3C, Dazhong Instruments, Shanghai, China). The scanning electron micrographs were taken with a scanning electron microscope (SEM, S-4800, Hitachi, Tokyo, Japan).

2.3 *Fabrication of the immunosensor*

Every ITO plate was cut into 10×50 mm^2 slides in this work, and 10×10 mm^2 slides was used as the

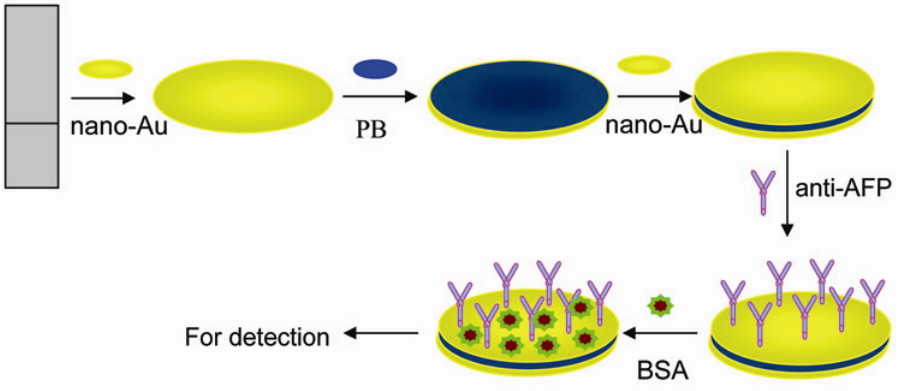

Scheme 1. Schematic diagram of the step-wise immunosensor fabrication process.

working surface, which was cleaned by sonication with acetone (10 min), dichloromethane (10 min), and water (2 min several times) one by one, as reported previously.[26,27] These clean slides were placed in a vial with a mixture of $H_2O : H_2O_2$ (30%) : NH_3 (25%) (5 : 1 : 1) and stirred at 70°C for 1 h. Then the slides were washed with plenty of water and dried for 4 h at 100°C.

The cleaned electrode was performed in 1% (m/v) $HAuCl_4$ + 0·1 mol L^{-1} KNO_3 by applying a constant potential of –0·2 V for 30 s to form a nano-Au monolayer. The modified electrode was carefully washed with water. The electro-deposition of PB on to the nano-Au-modified electrode was accomplished by applying a constant potential of 0·4 V for 40 s in the solution containing 2·0 mmol L^{-1} $FeCl_3$, 2·0 mmol L^{-1} $K_3[Fe(CN)_6]$, 0·1 mol L^{-1} KCl. Then, the modified electrode was carefully washed with water and electrochemically scanned for 15 times between –0·4 V and 0·4 V at 50 mV s^{-1} in 0·1 mol L^{-1} KCl/0·1 mol L^{-1} HCl solution. Following that, it was thoroughly rinsed with distilled water and was dried at 100°C for 1 h. Subsequently, the modified electrode was immersed in 1% (m/v) $HAuCl_4$ + 0·1 mol L^{-1} KNO_3 and applied constant potential –0·2 V for 30 s in order to form a nano-Au monolayer to prevent the leakage of PB. As control experiment, the assembly immunosensor was prepared as follows: the PB/nano-Au-modified ITO electrode was immersed in a gold nanoparticles solution overnight (about 12 h). Then, the resulting electrodes were immersed in an anti-AFP solution at 4°C over night. Finally, the modified immunosensors were incubated in 0.25% BSA solution about 2 h in order to block possible remaining active sites of the nano-Au monolayer and avoid the non-specific adsorption. The finished immunosensors were stored at 4°C when not in use. The schematic illustration of the LBL electro-deposition immunosensor was shown in scheme 1.

2.4 *Experimental measurements*

The electrochemical characteristics of the modified electrode were characterized by cyclic voltammetry (CV). Electrochemical experiments were performed in a conventional electrochemical cell containing a three-electrode arrangement. The CV scan was taken from –0·7 to 0·7 V with a sweeping rate of 50 mV s^{-1} in working buffer at 25 ± 0·5°C.

3. Results and discussion

3.1 *SEM characterization of electro-deposition nano-Au-modified ITO interfaces*

The scanning electron microscopy (SEM) was used to obtain the surface dynamic images of the nano-Au modified ITO after each electro-deposition period. The SEM images showed clearly the influence of the surface state of the ITO substrate on the morphology, size and density of the electrochemically formed nano-Au (figure 1). The electrolysis time periods chosen were 10 ~ 40 s. Figure 1a showed the image of bare ITO interface, which exhibited quite homogeneous and flat morphology. When electro-deposition for 10 s, flat and fringed tiles with almost circular shape and small gold sphere were appeared in the center, which were evidence of the presence of gold nanoparticles (figure 1b). For comparison, the diameter of nano-Au on the ITO (figure 1c) became larger than that in figure 1b, at deposition time 30 s. Meanwhile, the electro-

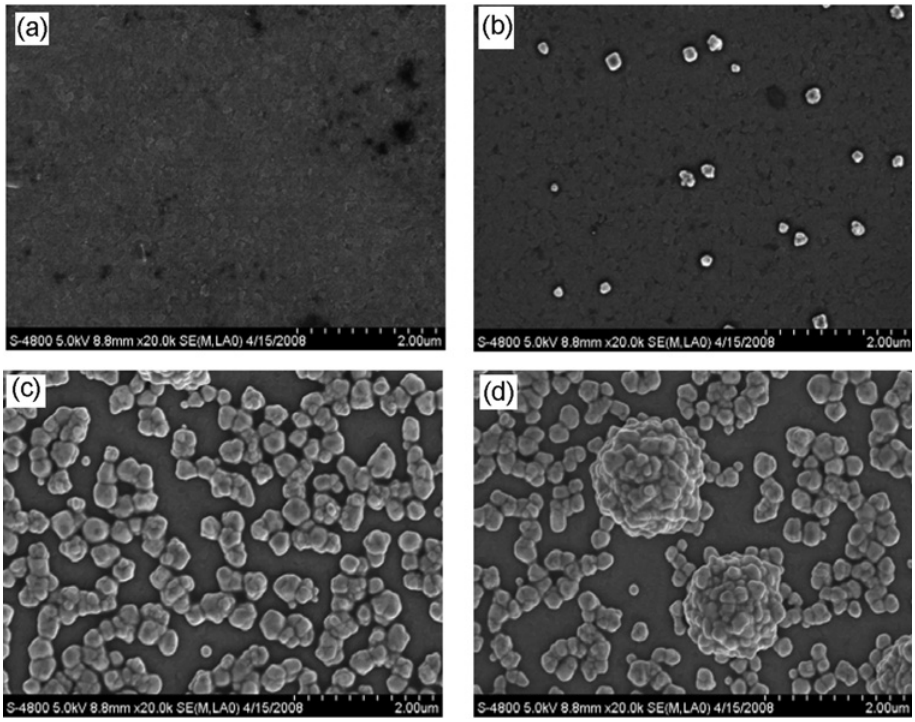

Figure 1. SEM images of (**a**) bare ITO, (**b**) electro-deposition nano-Au 10 s, (**c**) electro-deposition nano-Au 30 s, (**d**) electro-deposition nano-Au 40 s. Constant potential electrolysis was performed in 1% (w/v) $HAuCl_4$ and 0·1 M KNO_3 at E = –0·20 V SCE^{-1}.

deposited nano-Au showed a well-defined spherical structure and formed gold films which strongly resembled nano-Au formed on glass through chemical vapor deposition.[28] At 40 s, the gold spheres grew to triangular flower-like structures and the nano-Au particles grew and coalesced to longitudinal and curved 'blobs' (figure 1d). In this paper, deposition time 30 s was chosen for all the following experiments.

3.2 *Characteristics of electrochemistry on electrode surface*

Electrochemical impedance spectroscopy (EIS), a powerful electroanalytical technique to probe the electron transfer kinetics of modified electrodes,[29–31] has been successfully applied in immunoassay. The complex impedance included the sum of the real, $Z_{re}(\omega)$, and imaginary, $Z_{im}(\omega)$, componented originating mainly from the resistance and capacitance of the cell, respectively. The typical shape of an impedance spectrum included a semicircle portion at high frequencies, which corresponded to the electron-transfer limited process and a linear part at a low frequency range, which represented the diffusion-limited process. The insert (A) of figure 2 was the equivalent circuit, including the ohmic resistance of the electrolyte solution, R_s, the Warburg impedance, Z_w, the double layer capacitance, C_{dl}, and the electron-transfer resistance, R_{et}. R_s represented bulk properties of the electrolyte solution and Z_w represented diffusion feature of redox probe in solution. Therefore, these parameters were not affected by the electrochemical reaction occurring at the electrode surface. C_{dl} and R_{et} depended on the dielectric and insulating features at the electrode/electrolyte interface, respectively. When an electrode was modified, the modifier on electrode changed the double layer capacitance and electron-transfer resistance and the change can be obtained from the impedance spectra. By measuring the change of capacitance or electron-transfer resistance, the modifier on electrode can be detected indirectly. Therefore, each modification step of the electrode was characterized by EIS.

Figure 2 showed the EIS of the differently modified electrodes in PBS + 0·1 mol L^{-1} KCl + 5·0 mmol L^{-1} $Fe(CN)_6^{4-/3-}$. The probe implied the characteristic of a diffuse limiting step of the elec-

trochemical process on a bare ITO electrode (curve a). After being electrodeposited with nano-Au, the resistance of the film-modified electrode decreased (curve b), indicating a higher electron-transfer resistance at the electrode interface. The semicircle diameter decreased slightly with the {nano-Au/PB/nano-Au} multilayer film formation on the electrode (curves c and d), which can be attributed to the excellent electrochemical activity of PB, as well as the good conductivity of nano-Au. When the anti-AFP film were obtained in turn, the interfacial resistance increased, which were consistent with the fact that the hydrophobic layer of the protein insulated the conductive support and perturbs the interfacial electron transfer (curve e, in the insert (B) of figure 2).

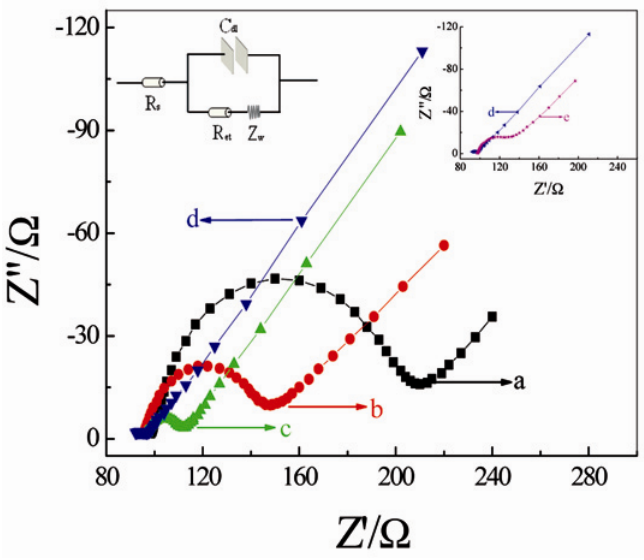

Figure 2. EIS of the different electrodes: a), bare ITO; b), nano-Au/ITO; c), PB/nano-Au/ITO; d), nano-Au/PB/nano-Au/ITO; e), anti-AFP/nano-Au/PB/nano-Au/ITO.

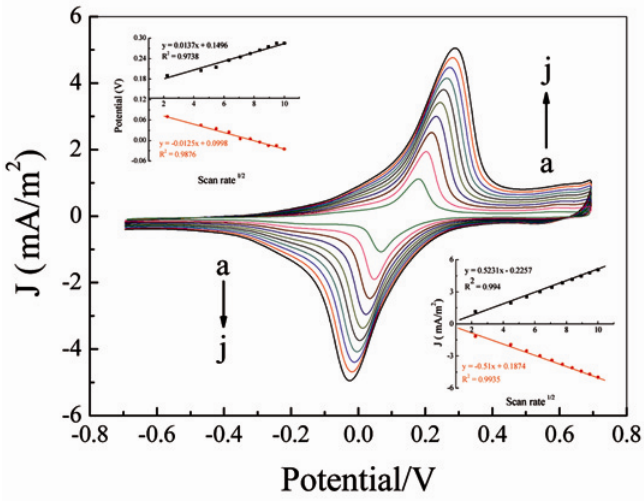

Figure 3. CVs of the modified electrode at different scan rates (from a to j): 5, 20, 30, 40, 50, 60, 70, 80, 90, 100 mV s^{-1} in 5 mL 0·1 mol L^{-1} PBS buffer solution (pH 6·5) under room temperature. All potentials are given vs SCE. The inset shows the dependence of redox peak currents on the potential sweep rates (the working surface was 10 × 10 mm^2).

The cyclic voltammogramms of the proposed immunosensor in PBS buffer solution at different scan rates ranging from 5 to 100 mV s^{-1} were investigated in figure 3. The anodic and cathodic peak currents were directly proportional to the square root of scan rate, as shown in the inset of figure 3, suggesting a diffusion-controlled behaviour.

3.3 *Optimization of the assay conditions*

The influence of the temperature on the current response was investigated at different temperatures ranging from 15 to 45°C, under the same experimental conditions of 50 ng mL^{-1} constant concentration AFP as the model (figure 4a). It was found that the current response decreased with the increasing of the temperature till 37°C, and the trend became to level off above 37°C, indicating that the immunocomplexes might have been destroyed over 37°C. However, considering the activity of biomoleculars and the life-time of biosensor, the room temperature 25 ± 0·5°C was used as incubation temperature.

The effect of incubation pH on amperometric response was also investigated with pH value change from 5·0 to 8·5 using 50 ng mL^{-1} constant concentration of AFP at 25°C. As shown in figure 4b, the current response increased with increasing pH value from 5·0 to 5·5, then the current response decreased as pH value increased further and the maximum response was obtained at pH 5·5. It is well-known that the activity of immunoproteins is inhibited at relatively low pH. So a pH 6·5 of incubation solution was selected as incubation pH for further studies.

3.4 *Comparative study of various immunosensors*

Comparative studies of the potential responses of different modified immunosensors were carried out in 5, 10, 25, 50, 100, 200, 300 ng mL^{-1} AFP under the same conditions. As shown in figure 5, curve b exhibited a less steep decline with a narrower linear response than curve a, which indicated that LBL electro-deposition immunosensors exhibited higher

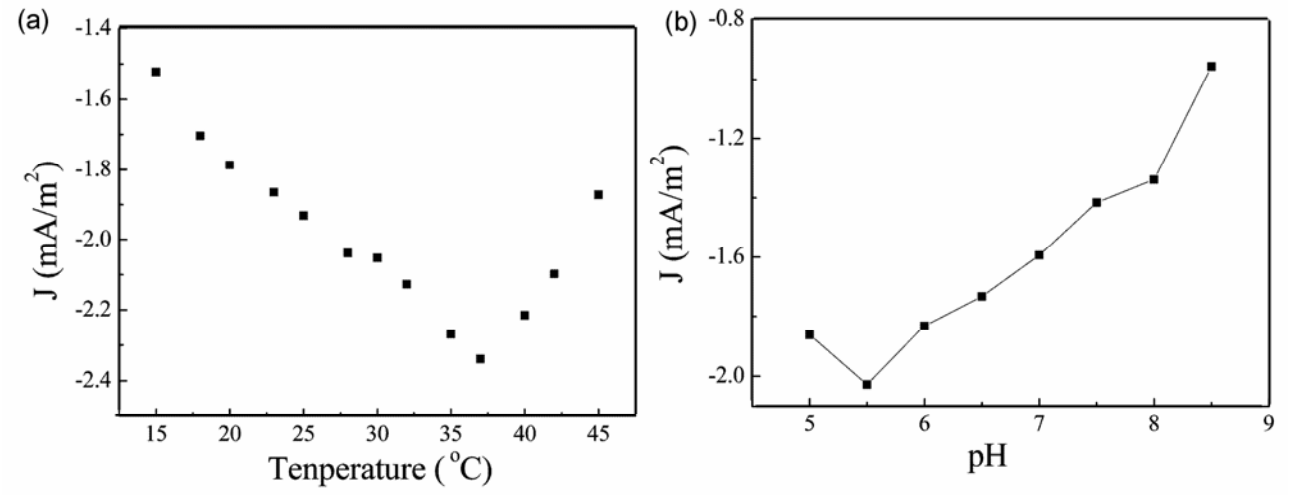

Figure 4. Effect of incubation parameters on immunoreaction: (**a**) incubation temperature; (**b**) incubation pH. CV determination was carried out in 0·1 mol L^{-1} PBS at 25°C, with scan rate 50 mV s^{-1} (the working surface was 10 × 10 mm^2).

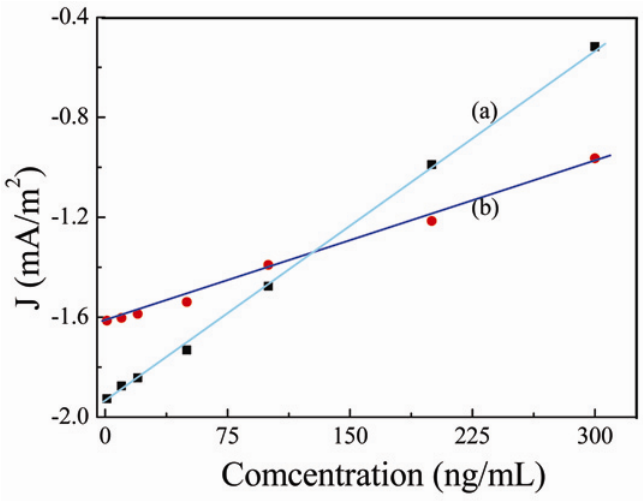

Figure 5. Potentiometric responses to different concentrations of AFP in pH 6·5 PBS (the working surface was 10 × 10 mm^2): a) LBL electro-deposition immunosensor, b) assembly immunosensor.

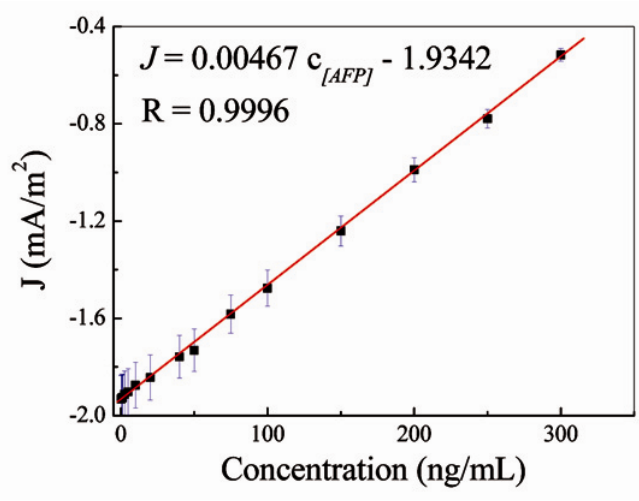

Figure 6. Calibration plots of the relationship between current response and AFP concentration. All the measurements were carried out in 0·1 mol L^{-1} phosphate buffer solution (pH 6·5) at 25°C for 15 min and the scan rate 50 mV s^{-1} (the working surface was 10 × 10 mm^2).

potential responses than that of the assembly immunosensors. The reason might be that electro-deposition nano-Au on the PB layer not only provided a microenvironment similar to that of the proteins in native systems to retain the activity of the proteins but also prevented the leakage of hydrosoluble PB, which enhanced the stability of the immunosenosr greatly. Thus, LBL electro-deposition immunosensor was chosen for the following experiments.

3.5 *Performance of the immunosensor*

Under optimal experimental conditions, the calibration plot for different concentrations of AFP detection with the proposed immunosensor is illustrated in figure 6. The cyclic voltammgramm peak currents of the resulted anti-AFP/nano-Au/PB/nano-Au/ITO after the antigen-antibody reaction decreased with the increase of AFP concentration. The calibration curve for the membrane immunosensor under opti-

Table 1. Part of the results of different methods applied in clinic serum test.

Sample number	AFP concentration (ng ml^{-1})		Relative error (%)
	The proposed immunosensor	ELISA	
1	10·8 ± 0·2	10·5 ± 0·1	2·9
5	26·2 ± 0·1	25·7 ± 0·3	1·9
15	49·8 ± 0·1	50·6 ± 0·2	–1·6
25	75·6 ± 0·3	74·1 ± 0·1	2·0
32	99·2 ± 0·3	100·3 ± 0·2	–1·1
40	150·4 ± 0·2	148·6 ± 0·1	1·2

mal experimental conditions showed a linear response to AFP. The concentration range covered from 0·25 to 300·0 ng mL^{-1} with a detection limit of 0·04 ng mL^{-1}. The linear regression equation was i = 0·0467 $c_{[AFP]}$ – 19·342 and correlation coefficient of 0·9996 (figure 6). It was observed that hydrosoluble PB was a good electron mediator, which had good reversibility of the electrode reaction process. Electro-deposition nano-Au on the PB layer not only prevented the leakage of PB so as to enhance the stability of the immunosenosr greatly, but also provided a microenvironment.

3.6 *Selectivity and stability of the immunosensor*

The selectivity was one of the potential advantages of using biological molecules as recognition elements in biosensors. The effect of possible interferents on the response of the developed immunosensor was studied. The interference substances included carcinoembryonic antigen, human IgG, hepatitis B surface antigen, hepatitis B core antigen, hepatitis B surface antigen, ascorbic acid, L-cysteine, L-lysine, L-glutamate. The interferential degree of the substance can be examined by detecting the amperometric responses. The imunosensors were separately exposed to 50 ng mL^{-1} AFP solution with interference and without interference. The responses of cyclic voltammgramms in the two solutions did not show remarkable difference. The results showed that the proposed immunosensor based on the highly specific antigen-antibody immunoreaction had a good selectivity to AFP.

The stability of the successive assays was studied by 100 cycles CV measurements in working buffer after being incubated with 50 ng mL^{-1} AFP, a 2·7% decrease of the initial response was observed. The long-time stability of the immunosensor was also investigated over a 60 days period. The immunosensor was stored at 4°C and measured every 5 days. It was found that there were no apparent changes of the current response, 7·6% RSD yield. The good stability may be due to the fact that nano-Au/PB/nano-Au was stable and anti-AFP molecules were attached firmly onto the surface of nano-Au monolayer.

3.7 *Preliminary application of immunosensor in human serum*

In order to investigate the feasibility of the proposed method, the immunosensor was applied to the analysis of human serum for clinical diagnosis. The results with 40 human serum samples obtained from the immunosensor were compared with those from an established ELISA technique, which were shown in table 1. A good correlation was found between the results of the two methods with the range of 8·7–7·2%. Thus, the proposed method may be extended to the determination of AFP in human serum.

4. Conclusions

In this work, a new amperometric immunosensor was described for the determination of AFP with good sensitivity and high stability based on the {nano-Au/PB/nano-Au} multilayer film by the LBL electro-deposition of nano-Au and PB. The studied immunosensor had several attractive advantages, such as high stability of {nano-Au/PB/nano-Au} multilayer film, easily adsorptive immobilization of antibody on nano-Au monolayer, and the use of ITO instead of gold electrode, glassy carbon electrode and platinum electrode etc, to construct a new disposable amperometric immunosensor with good sensitivity and high stability, as well as the simplicity of use and cost effectiveness. Although the strategy has only been applied to anti-AFP and AFP

as a model system, it could be readily extended toward the determination of other clinically or environmentally interested biospecies.

Acknowledgements

This work was supported by the National Natural Science Foundation of China (No. 30200264, 30571863), the National Science Foundation of Chongqing City (CSTC-2006BB5117), China.

References

1. Li T-X 2001 *Modern clinical immunoassay* (Beijing: Military Medical Science Press)
2. Bader D, Riskin A, Vafsi O, Tamir A, Peskin B, Israsel N, Merksamer R, Dar H and David M 2004 *Clin. Chim. Acta* **349** 15
3. Chuang L, Hwang J-Y, Chang H-C, Chang F-M and Jong S-B 2004 *Clin. Chim. Acta* **348** 87
4. Stefanova I and Horsjsi V 1988 *J. Immunol. Met.* **111** 67
5. Bisceglie A, Sterling R, Chung R, Everhart J, Dienstag J and Bonkovsky H 2005 *J. Hepatol.* **43** 434
6. Fu Z-F, Hao C, Fei X-Q and Ju H-X 2006 *J. Immunol. Methods* **312** 61
7. Chen C-H, Huang G-T, Yang P-M, Chen P-J, Lai M-Y, Chen D-S, Wang J-D and Sheu J-C 2006 *Eur. J. Cancer* **42** 2524
8. Wang Y-Y, Luo J, Zhu M-W, Liu L-N and Ma X 2006 *Inter. J. Gynecol. Obstet.* **94** 67
9. Matsuya T, Tashiro S, Hoshino N, Shibata N, Nagasaki Y and Kataoka K 2003 *Anal. Chem.* **75** 6124
10. Wang G-L, Yuan J-L, Gong B-L, Matsumoto K and Hu Z-D 2001 *Anal. Chim. Acta* **448** 165
11. Belanger L, Sylvestre C and Dufour D 1973 *Clin. Chim. Acta* **48** 15
12. Aguilar Z P, Vandaveer W R and Fritsch I 2002 *Anal. Chem.* **74** 3321
13. Wang J 2006 *Biosens. Bioelectron.* **21** 1887
14. Calvo E J, Danilowicz C and Lagier C M 2004 *Biosens. Bioelectron.* **19** 1219
15. Zacco E, Pividori M I and Llopis X 2004 *J. Immunol. Methods* **286** 35
16. Hayashi K, Iwasaki Y, Horiuchi T, Sunagawa K and Tate A 2005 *Anal. Chem.* **77** 5236
17. Zhang J-D, Kambayashi M and Oyama M 2005 *Electroanalysis* **17** 408
18. Sun X-H and Gillis K D 2006 *Anal. Chem.* **78** 2521
19. Tominaga M, Kumagai T, Takita S and Taniguchi I 1993 *Chem. Lett.* **22** 1771
20. Qiu H-B, Yan J-L, Sun X-H, Liu J-F, Cao W-D, Yang X-R and Wang E-K 2003 *Anal. Chem.* **75** 5435
21. Zheng D, Wang N, Wang F-Q, Dong D, Li Y-G, Yang X-Q, Guo L-H and Cheng J 2004 *Anal. Chim. Acta* **508** 225
22. Zhan W, Alvarez J and Crooks R M 2002 *J. Am. Chem. Soc.* **124** 13265
23. Chen Z-P, Jiang J-H, Shen G-L and Yu R-Q 2005 *Anal. Chim. Acta* **553** 190
24. Enustun B V and Turkevich J J 1963 *J. Am. Chem. Soc.* **85** 3317
25. Ferri T, Poscia A and Santucci R 1998 *Bioelectrochem. Bioenerg.* **44** 177
26. Corry B, Uilk J and Crawley C 2003 *Anal. Chim. Acta* **496** 103
27. Markovich I and Mandler D 2001 *J. Electroanal. Chem.* **500** 453
28. Ruach-Nir I, Bendikov T, Doron-Mor I, Barkay Z, Vaskevich A and Rubinstein I 2007 *J. Am. Chem. Soc.* **129** 84
29. Cui X-L, Jiang D-L, Diao P, Li J-X, Tong R-T and Wang X-K 1999 *J. Electroanal. Chem.* **470** 9
30. Foschini C R, Souza D P F, Paulin Filho P I and Varela A 2001 *J. Eur. Ceram. Soc.* **21** 1143
31. Sundfors F, Bobacka J, Ivaska A and Lewenstam A 2002 *Electrochim. Acta* **47** 2245